Published in final edited form as:

Biochem Biophys Res Commun. 2022 June 18; 609: 163–168. doi:10.1016/j.bbrc.2022.03.161.

Attenuated cell-cycle division protein 2 and elevated mitotic roles of polo-like kinase 1 characterize deficient myoblast fusion in peripheral arterial disease

Ricardo Ferrari[1], **Guangzhi Cong**[1,2], **Ansuman Chattopadhyay**[3], **B Xie**[1], **E Assaf**[1], **K Morder**[1], **Michael J Calderon**[4], **Simon C Watkins**[4], **Ulka Sachdev**[1]

[1]·University of Pittsburgh Medical Center Department of Surgery, Division of Vascular Surgery

[2]·Department of Cardiology, Cardiovascular Institute, General Hospital of Ningxia Medical University, Yinchuan, Ningxia, China (Visiting Scholar at 1 from 1/2018 to 11/2020)

[3]·Health Sciences Library System, University of Pittsburgh School of Medicine

[4]·Center for Biologic Imaging @ University of Pittsburgh

Abstract

Introduction: We propose that MuSC-derived myoblasts in PAD have transcriptomic differences that can highlight underlying causes of ischemia-induced myopathy.

Methods: Differentiation capacity among perfused and ischemic human myoblasts was compared. Following next generation sequencing of mRNA, Ingenuity Pathway Analysis (IPA) was performed for canonical pathway enrichment. Live cell imaging and immunofluorescence were performed to determine myocyte fusion index and protein expression based on insights from IPA, specifically concerning cell cycle regulators including cell-division cycle protein 2 (CDC2) and polo-like kinase 1 (PLK1).

Results: Ischemic myoblasts formed attenuated myotubes indicative of reduced fusion. Additionally, myoblasts from ischemic segments showed significant differences in canonical pathways associated with PLK1 (upregulated) and G2/M DNA damage checkpoint regulation (downregulated). PLK1 inhibition with BI2536 did not affect cell viability in any group over 24 hours but deterred fusion more significantly in PAD myoblasts. Furthermore, PLK1 inhibition reduced the expression of checkpoint protein CDC2 in perfused but not ischemic cells.

Conclusion: Differentiating myoblasts derived from ischemic muscle have significant differences in gene expression including those essential to DNA-damage checkpoint regulation and cell cycle progress. DNA-damage checkpoint dysregulation may contribute to myopathy in PAD.

Keywords

Peripheral arterial disease; myopathy; ischemia; polo-like kinase; cell cycle regulation; RNA sequencing

Please Address All Correspondence to: Ulka Sachdev, MD, Associate Professor of Surgery, Magee Womens Hospital of UPMC 300 Halket Street Suite 5414, Pittsburgh, PA 15213, Sachdevu2@upmc.edu, 412-802-3036.

Introduction:

Peripheral arterial disease (PAD) is a disease affecting millions in the United States and can lead to limb loss [1,2]. Experimental research in the field has commonly been focused on improving angiogenesis [3–5], while less has evaluated how to improve muscle function. Recent studies have shown that men suffering from PAD exhibit sarcopenia, which is a reflection not only of ischemic pain, but also of myopathic damage [6]. PAD also causes biochemical changes within the muscle tissue itself [7–10]. Indeed, even intermittent claudication which is typically managed medically may have untoward effects on muscle function despite normal resting perfusion [11].

MuSC are a small population of cells that are quiescent in skeletal muscle and reside between the sarcolemma and basal lamina [12]. Following injury, they can differentiate into myoblasts, divide, fuse into multinucleated myocytes and join to pre-existing fibers to promote repair [13]. We hypothesized that in PAD, myoblasts isolated from ischemic skeletal muscle have deterred myogenic potential contributing to myopathy. We identified pathways affecting myoblast differentiation, and modulated targets to assess the effects.

Methods:

Human Subjects:

Ethical considerations ––—Human subjects research followed the guidelines of the Declaration of Helsinki. Tissue collection was performed under the auspices of the Institutional Review Board of the University of Pittsburgh. The collection of tissue from de-identified amputation specimens met criteria for exemption under section 45 CFR 46.102(f) (#Study PRO11070041). Tissue procurement for perfused PAD muscle was obtained under the protocol #Study19050272. Written consent was obtained from these patients.

Patient Samples ––—Ischemic myoblasts were harvested from transtibial or transfemoral amputation procedures for advanced, noninfected PAD. The diagnosis of PAD was determined based on an ankle-brachial index (ABI) < 0.8, toe pressure < 50mmHg and/or angiographic evidence of atherosclerotic occlusive disease involving the superficial femoral, popliteal and/or tibial vessels of the ipsilateral leg. Patient age, gender, race and prior vascular interventions were recorded. Perfused myoblasts were obtained from muscle segments with normal pulse volume recordings. Additionally, myoblasts from healthy donors without PAD were obtained from Cook MyoSite (Pittsburgh, PA).

Myoblast Isolation:

Ischemic myoblasts were harvested as described [14]. Two to three grams of tissue were removed from the ischemic *tibialis anterior* (TA) muscle within 3 cm of the tibial tuberosity (proximal) and the lateral malleolus (distal). Perfused myoblasts were taken from segments of *vastus medialis and lateralis* of the guadriceps. Muscle was minced in 1ml of Hank's Balanced Salt Solution (HBSS; Gibco, #14175-095). The resulting slurry was centrifuged for 5 minutes and homogenized using dispase II (1.2 U/ml; Roche Diagnostics, #11088882001) and collagenase D (5mg/ml; Sigma, # D4693-1G). Following

incubation at 37°C and 5% CO_2 myoblasts were obtained using a modified pre-plating technique as described [15]. Briefly, rapidly adhering cells were discarded, while the slowest fractions to adhere were kept for further isolation. During isolation, cells were maintained in a low-glucose medium containing 16% Fetal Bovine Serum (FBS; Gibco, #16140071), fetuin, 7.5% bovine serum albumin (BSA; Sigma, #A8412), dexamethasone (Sigma, #D8893), gentamicin (Gibco, #15750-060), human Epidermal Grow Factor (hEGF; Gibco, #PHG0311) and fungizone (Gibco, #15290-018) which was replaced every 48 hours to minimize cell disruption. Slow-adhering fractions of cells were sequentially removed and subjected to two rounds of magnetic assisted cell sorting (MACS; Miltenyi Biotech, #130-090-312; MS Columns, #130-042-201) with anti- CD56-conjugated magnetic beads (Miltenyi Biotech, #130-050-401) [16]. Myoblasts (Pax7−/MyoD+) were quantified using immunocytochemical techniques identifying MyoD1 (Abcam, #ab64159) while fibroblast contamination was identified by identifying TE-7 (Milipore, #3112589) [16].

Myogenicity studies and imaging:

Incucyte® live cell imaging ––Myoblasts were seeded in a collagen pre-coated 96-well clear bottom plate (10,000cells/well; Corning, #3610) overnight with medium supplemented with 16% fetal-bovine serum. To assess myocyte tube formation, cells were then incubated with Incucyte® CytoLight Red Lentivirus (EF-1 Alpha Promoter, Puromycin selection, Sartorius #4482) in reduced serum. Plates were placed into the IncuCyte® Live-Cell Analysis System SX5 and warmed to 37°C for 30 minutes prior to scanning. Cells were imaged in phase contrast and red or green fluorescence with a 20x objective every 2 hours for a total of 120h. Incucyte® Controller Version 2020A software quantified tube formation and length (Cat. No. 9600-0011).

Myoblast proliferation ––A total $1x10^4$ cells were plated in 96 well plates. After 72 hours, CellTiter-Glo Luminescence cell viability assay reagent (Promega, ct. no. G7570) was added to each well, and incubated in RT for 10 minutes. The relative luminescence was measured using a Biotek microplate reader.

Myoblast differentiation (static) ––Twenty thousand cells were plated on chamber slides (MatTek, Ashland, MA #P35GCol-1.5-10-C) and allowed to differentiate over 5 days in culture media supplemented with 2% FBS, which promotes myoblast differentiation [17]. After washing, cells were fixed, permeabilized and incubated with antibodies to MF20 10ug/ml (R&D systems, MAB4470) to identify myosin-heavy chain 2 (MHC2) as well as DAPI (1:1000) to identify nuclei. Cells were imaged using an Olympus Fluoview 1000 confocal microscope at 20x magnification. Myocyte fusion index (MFI) was calculated by dividing the total number of nuclei within multinucleated myocytes (>2 nuclei) by the total number of nuclei in the image [15]. In some experiments, cells were exposed to BI2356, a polo-like kinase 1 (PLK1) inhibitor used in chemotherapeutic regimens for esophageal cancer [18]. Calculations assessing differentiation or proliferation were performed in triplicate and expressed as means +/− standard error of the mean (SEM). Differences in proliferation and MFI were determined using Student's t-test comparing two groups with continuous means, and analysis of variance with Holms-Sidak *post hoc* analysis for more than two groups. Experiments were repeated a minimum of three times.

Immunofluorescence -—Cells were seeded on MatTek dishes as described above, fixed and permeabilized. Cells were then exposed to primary antibodies targeting PLK1 (Invitrogen, Cat#MA1-848) and cell-division cycle protein 2 (CDC2; Cell Signaling, Cat#9116S). Following washing and incubation with fluorescence conjugated secondary antibodies (Abcam, Cat#150117) cells were imaged using confocal microscopy as described for differentiation.

Immunoblotting -—MuSC were lysed in phenylmethanesulfonyl fluoride (PMSF) and protein content quantified with bicinchoninic acid, loaded on to SDS-PAGE gels, and transferred onto nitrocellulose membranes. Immunoblots were probed with antibodies to PLK1 and CDC2 (shown above). Additionally, we evaluated expression of CDC25 (R&D Systems, #MAB1648), which can induce cells to enter mitosis by PLK1.[19] Horse-radish peroxidase based chemiluminescence was used to detect protein expression. Image J analysis program was for semi-quantitative analysis of each protein normalized to GAPDH.

Transcriptomic analysis:

RNA extraction and quality control -—Myoblasts underwent RNA sequencing after 24 hours of proliferation as well as 5 and 10 days of differentiation. RNA was extracted using Qiagen RNA extraction kits (Qiagen; RNeasy Plus Mini Kit, #74134). Libraries were prepared with the TruSeq stranded mRNA kit (Illumina # 20020595) following the manufacturer's protocol. Briefly, mRNA was purified using oligo-dT magnetic beads from 100ng – 1μg total RNA. Following two rounds of purification, mRNA was fragmented. First strand reverse transcription was performed with polydT primers. After second strand synthesis, blunt ended cDNA fragments were A-tailed followed by ligation of indexed sequencing adapters. PCR amplification provided selective enrichment of DNA with adapters ligated to both ends and was followed by library quantity and quality assessment by fluorometric assays (Qubit, Thermo-Fischer) and Agilent DNA 1000 TapeStation 4200 (Agilent Technologies, Inc. 2019) assays, respectively. Flowcells for the NextSeq 500 were seeded with 1.8pM denatured library for automated cluster formation and 2 x 75 paired end sequencing. 30-40 million reads were obtained/conducted per sample.

RNA Sequencing Data Processing and Alignment -—RNA sequence reads were analyzed using a reference-based mapping strategy implemented in CLC Genomics Workbench (V.12.0.3; https://digitalinsights.qiagen.com). After quality control, adapter trimming, quality filtering, and per-read quality running, the "cleaned" reads were aligned to the GRCh38 human genome reference (www.ncbi.nlm.nih.gov/assembly/GCF_000001405.39). Principal component analysis (PCA), Venn diagram creation, and heat-map generation were performed sequentially. Empirical analysis identified differentially expressed genes (DEGs) with default parameters. DEGs were then filtered according to pairwise comparisons for biological significance (absolute log-2 FC [ABS(Log2FC)] > 1) and statistical significance with a false discovery rate (FDR) $p < 0.05$. [20]

Bioinformatics and Statistical Analyses of DEG -—Pathway enrichment analysis and visualization were performed with Ingenuity Pathway Analysis (IPA; QIAGEN Inc.,

https://www.qiagenbio-informatics.com/products/ingenuity-pathway-analysis) [21]. Briefly, IPA regulation z-score algorithms were used to determine the activation state of canonical pathways and upstream regulators using the general molecular network implemented in the IPA Knowledge Base [22]. To enhance the stringency of our analysis, only z-scores with two-fold positive or negative differences (> 2 or < −2) were considered significant. The likely consequence of DEGs on downstream canonical biological processes, phenotypes, and disease states were predicted.

Results and Discussion:

Myoblast fusion in cells derived from ischemic muscle in PAD patients is deterred when compared to those from perfused muscle.

We first used real-time live cell imaging to evaluate myocyte fusion capacity in ischemic and perfused myoblasts over time. Cytoplasmic stains allowed for the visualization of cell structure while specialized software calculated the total length of myotubes formed. Figure 1 demonstrates final tube formation (Figure 1A, B) and the average tube length change over time. PAD myoblasts demonstrated diminished overall myotube length after approximately 4 days when compared to those obtained from healthy donors (Figure 1C). However, cell proliferation was higher in ischemic PAD cells than in perfused cells following 72 hours of culture (Figure 1D).

Unbiased transcriptomic analysis demonstrates significant differences between ischemic and healthy donor myoblasts during differentiation:

We performed RNA sequencing coupled with pathway analysis to determine if differentially expressed genes (DEG) might explain the deficit in myocyte fusion. Figures 2A–C demonstrates Volcano plots showing the number of DEGs at each timepoint while Figure2D illustrates similar data by PCA analysis. In the absence of a differentiation stimulus, PAD and control cells had fewer DEG, suggesting that at rest, cells had similar expression. However, the number of DEGs between control and PAD cells greatly increased following five days of differentiation, particularly in cells taken from proximal TA.

Mitotic-roles of polo-like kinase 1 (PLK1) and G2/M DNA damage checkpoint pathways differed significantly between ischemic and healthy donor myoblasts:

To understand pathways related to DEGs between healthy and ischemic PAD myoblasts in an unbiased fashion, we performed IPA on the transcriptomic data. Strikingly, in both proximal and distal ischemic PAD cells, pathways associated with the mitotic role of PLK1 were significantly upregulated (z-scores: proximal 13.0>z<14.0, distal 8.0>z<8.5). Concomitantly, pathways associated with the G2/M DNA damage checkpoint were significantly downregulated in those same cell groups (z-scores: proximal 9.0>z<10.0, distal z 6.5>z<7.0). The G2/M DNA damage checkpoint of which CDC2 is a key component, is a critical regulator of cell cycle progression, and is regulated by PLK1.[23] PLK1 activation promotes expression and activation of CDC2, allowing for cells to progress from G2 to M in the absence of DNA damage.[24] However, PLK1 activity can also suppresses G2/M DNA damage checkpoint functions allowing mitosis to progress even if cell or DNA damage is present [25–27]. This can occur through activation of CDC25 which also regulates and

induces mitosis.[19] Indeed, the actions of PLK1 can promote cell survival in cancer and is a target for chemotherapeutic agents [28]. In muscle, PLK1 activity has been shown to be critical for embryonic myogenesis and adult muscle regeneration during injury in a mouse model. [29] However, unlike CDC2, overexpression of PLK1 is not sufficient to increase cell division in cardiomyocytes. [30] Loss of PLK1 is seen with differentiation into mature myocytes[30]; thus, persistent activity associated with PLK1 during active differentiation suggests abnormal fusion capacity.

Immunofluorescent detection of DNA damage checkpoint protein CDC2 expression is diminished in PAD and unresponsive to PLK1 inhibition:

The IPA demonstrated a striking upregulation of pathways associated with mitotic roles of PLK1 in PAD muscle cells which was related to downregulation of G2/M DNA damage checkpoint activity. We confirmed the presence of proteins associated with the G2/M DNA damage checkpoint. Both PLK1 and CDC2 were present in ischemic and perfused cells by immunoblotting. Importantly, CDC25 which is can be activated by PLK1 was elevated in ischemic myoblasts (Figure 3A). To further confirm expression patterns within cells using immunofluorescence, we evaluated the expression of both PLK1 and CDC2 in both ischemic (proximal and distal TA) and perfused (quadriceps) myoblasts in PAD that were not differentiated into myotubes. By doing so, we were able to use perfused and ischemic muscle cells that were harvested in a similar manner from PAD patients. PLK1 did not differ among the groups (Figure 3B). However, CDC2 expression by immunofluorescence was significantly reduced in ischemic compared to perfused myoblasts (Figures 3C,D). Additionally, in perfused myoblasts, CDC2 expression expectedly decreased with inhibition of PLK1 with BI2536. In contrast, in PAD cells from ischemic TA muscle, inhibition of PLK1 did not affect expression of CDC2. Thus, in perfused cells, CDC2 and PLK1 expression were positively correlated. In ischemic cells, CDC2 expression was attenuated and did not respond to modulation of PLK1, potentially affecting fusion capacity.

PLK1 inhibition attenuates myocyte fusion capacity in PAD:

We tested the hypothesis that PLK1 may be an important driver of myotube fusion particularly in the absence of CDC2. We therefore exposed cells to PLK1 inhibition with BI2536. Cells for all groups were viable following exposure to the inhibitor at 24 hours (Figure 4A) suggesting that the relatively diminished CDC2 expression and inhibition of PLK1 did not immediately kill cells. While pathways controlling mitosis have been shown to be redundant, [31] differentiation utilizes alternative mechanisms than those associated with mitosis. After five days of differentiation with and without BI2536, myocyte fusion remained intact in perfused healthy donor cells, but not in ischemic cells (Figure 4).

Our results suggest that PLK1 may have an important role in promoting myocyte fusion in cells injured by chronic ischemia. Its role in uninjured cells appeared less critical. In ischemic muscle disease, PLK1 may provide an important mechanism for cells to remain functional to promote muscle regeneration in the absence of CDC2. In support of this, recent literature suggests that PLK1 promotes post-natal myogenesis and MuSC survival following injury [29]. Our data has important implications for a wide group of people including those patients with PAD who require PLK1 inhibition for cancer. Cancer and PAD tend to affect

the same age of patients [32] and PLK1 inhibition causes significant muscle wasting in patients who are already at risk for sarcopenia. Our data also implies that chronic ischemia alters important cell cycle regulatory proteins that drive regeneration.

Our study has several strengths. The most notable is our ability to study human tissue from subjects with disease, increasing relevance for potential therapeutic targets. We also utilized RNA sequencing in an unbiased format and used results to inform further study. However, the study also has important limitations. We used controls from a commercial source as well as those from perfused segments of muscle in PAD patients. Both cell types have benefits – commercial cells are from donors without PAD and perfused cells from PAD patients were harvested similarly to our experimental ischemic cells. In separate studies, we demonstrated that the proliferative and fusion capacity as well as MyoD expression were similar between both groups (data not shown). Additionally, this study is not powered to account for effects of underlying medical conditions including diabetes that might have on our results. Despite these limitations, we were able to determine that the process of differentiation in PAD is compromised, which may underscore the myopathy seen in ischemic muscle disease. This appears to be at least in part due to differences in cell-cycle related pathways.

In summary, we have determined that ischemic myoblasts from PAD and those from perfused or healthy muscle donors differ significantly regarding pathways related to PLK1 and G2/M DNA damage checkpoints. PLK1 plays an important role in ischemic myoblast differentiation in the setting of diminished CDC2 expression. Unbiased approaches to myogenicity may help determine targets to improve muscle function in PAD.

Acknowledgements:

We would like to acknowledge Debbie Hollingshead, Bryan Thomson, Jeanette Lamb of the Genomics Research Core for Health Sciences Research @ Children's Hospital of Pittsburgh for their support in RNA sequencing data.

Funding:

This work was supported by the National Institutes of Health [grant numbers R01HLI36556 to US]

References

[1]. Selvin E, Erlinger TP, Prevalence of and risk factors for peripheral arterial disease in the United States: results from the National Health and Nutrition Examination Survey, 1999-2000, Circulation 110 (2004) 738–743. 10.1161/01.CIR.0000137913.26087.F001.CIR.0000137913.26087.F0 [pii]. [PubMed: 15262830]

[2]. Pavlovic S, Wiley E, Guzman G, Morris D, Braniecki M, Marjolin ulcer: an overlooked entity, International Wound Journal 8 (2011) 419–424. 10.1111/j.1742-481X.2011.00811.x. [PubMed: 21585661]

[3]. Biscetti F, Straface G, De Cristofaro R, Lancellotti S, Rizzo P, Arena V, Stigliano E, Pecorini G, Egashira K, De Angelis G, Ghirlanda G, Flex A, High-Mobility Group Box 1 Protein Promotes Angiogenesis after Peripheral Ischemia in Diabetic Mice through a VEGF-dependent Mechanism, Diabetes. db09–1507 [pii] 10.2337/db09-1507.

[4]. Kajiguchi M, Kondo T, Izawa H, Kobayashi M, Yamamoto K, Shintani S, Numaguchi Y, Naoe T, Takamatsu J, Komori K, Murohara T, Safety and efficacy of autologous progenitor cell transplantation for therapeutic angiogenesis in patients with critical limb ischemia, Circ J 71 (2007) 196–201. JST.JSTAGE/circj/71.196 [pii]. [PubMed: 17251666]

[5]. Powell RJ, Dormandy J, Simons M, Morishita R, Annex BH, Therapeutic angiogenesis for critical limb ischemia: design of the hepatocyte growth factor therapeutic angiogenesis clinical trial, Vasc Med 9 (2004) 193–198. [PubMed: 15675184]

[6]. Addison O, Prior SJ, Kundi R, Serra MC, Katzel LI, Gardner AW, Ryan AS, Sarcopenia in Peripheral Arterial Disease: Prevalence and Effect on Functional Status, Arch Phys Med Rehabil 99 (2018) 623–628. 10.1016/j.apmr.2017.10.017. [PubMed: 29138051]

[7]. Parmenter BJ, Raymond J, Dinnen PJ, Lusby RJ, Fiatarone Singh MA, Preliminary evidence that low ankle-brachial index is associated with reduced bilateral hip extensor strength and functional mobility in peripheral arterial disease, J Vasc Surg 57 (2013) 963–973 e961. 10.1016/j.jvs.2012.08.103. [PubMed: 23246081]

[8]. Schieber MN, Hasenkamp RM, Pipinos II, Johanning JM, Stergiou N, DeSpiegelaere HK, Chien JH, Myers SA, Muscle strength and control characteristics are altered by peripheral artery disease, J Vasc Surg 66 (2017) 178–186 e112. 10.1016/j.jvs.2017.01.051. [PubMed: 28647034]

[9]. Koutakis P, Miserlis D, Myers SA, Kim JK, Zhu Z, Papoutsi E, Swanson SA, Haynatzki G, Ha DM, Carpenter LA, McComb RD, Johanning JM, Casale GP, Pipinos II, Abnormal accumulation of desmin in gastrocnemius myofibers of patients with peripheral artery disease: associations with altered myofiber morphology and density, mitochondrial dysfunction and impaired limb function, J Histochem Cytochem 63 (2015) 256–269. 10.1369/0022155415569348. [PubMed: 25575565]

[10]. Koutakis P, Myers SA, Cluff K, Ha DM, Haynatzki G, McComb RD, Uchida K, Miserlis D, Papoutsi E, Johanning JM, Casale GP, Pipinos II, Abnormal myofiber morphology and limb dysfunction in claudication, J Surg Res 196 (2015) 172–179. 10.1016/j.jss.2015.02.011. [PubMed: 25791828]

[11]. Gasparini M, Sabovic M, Gregoric ID, Simunic B, Pisot R, Increased fatigability of the gastrocnemius medialis muscle in individuals with intermittent claudication, Eur J Vasc Endovasc Surg 44 (2012) 170–176. 10.1016/j.ejvs.2012.04.024. [PubMed: 22658608]

[12]. Charge SB, Rudnicki MA, Cellular and molecular regulation of muscle regeneration, Physiol Rev 84 (2004) 209–238. 10.1152/physrev.00019.2003 84/1/209 [pii]. [PubMed: 14715915]

[13]. Dumont NA, Bentzinger CF, Sincennes MC, Rudnicki MA, Satellite Cells and Skeletal Muscle Regeneration, Compr Physiol 5 (2015) 1027–1059. 10.1002/cphy.c140068. [PubMed: 26140708]

[14]. Spinazzola JM, Gussoni E, Isolation of Primary Human Skeletal Muscle Cells, Bio Protoc 7 (2017). 10.21769/BioProtoc.2591.

[15]. Lee JY, Qu-Petersen Z, Cao B, Kimura S, Jankowski R, Cummins J, Usas A, Gates C, Robbins P, Wernig A, Huard J, Clonal isolation of muscle-derived cells capable of enhancing muscle regeneration and bone healing, J Cell Biol 150 (2000) 1085–1100. 10.1083/jcb.150.5.1085. [PubMed: 10973997]

[16]. Agley CC, Rowlerson AM, Velloso CP, Lazarus NR, Harridge SD, Human skeletal muscle fibroblasts, but not myogenic cells, readily undergo adipogenic differentiation, J Cell Sci 126 (2013) 5610–5625. 10.1242/jcs.132563. [PubMed: 24101731]

[17]. Nehlin JO, Just M, Rustan AC, Gaster M, Human myotubes from myoblast cultures undergoing senescence exhibit defects in glucose and lipid metabolism, Biogerontology 12 (2011) 349–365. 10.1007/s10522-011-9336-5. [PubMed: 21512720]

[18]. Wu M, Wang Y, Yang D, Gong Y, Rao F, Liu R, Danna Y, Li J, Fan J, Chen J, Zhang W, Zhan Q, A PLK1 kinase inhibitor enhances the chemosensitivity of cisplatin by inducing pyroptosis in oesophageal squamous cell carcinoma, EBioMedicine 41 (2019) 244–255. 10.1016/j.ebiom.2019.02.012. [PubMed: 30876762]

[19]. Lobjois V, Jullien D, Bouché J-P, Ducommun B, The polo-like kinase 1 regulates CDC25B-dependent mitosis entry, Biochimica et Biophysica Acta (BBA) - Molecular Cell Research 1793 (2009) 462–468. 10.1016/j.bbamcr.2008.12.015. [PubMed: 19185590]

[20]. McCarthy DJ, Chen Y, Smyth GK, Differential expression analysis of multifactor RNA-Seq experiments with respect to biological variation, Nucleic Acids Res 40 (2012) 4288–4297. 10.1093/nar/gks042. [PubMed: 22287627]

[21]. Freeberg MAT, Easa A, Lillis JA, Benoit DSW, van Wijnen AJ, Awad HA, Transcriptomic Analysis of Cellular Pathways in Healing Flexor Tendons of Plasminogen Activator Inhibitor 1 (PAI-1/Serpine1) Null Mice, J Orthop Res (2019). 10.1002/jor.24448.

[22]. Krämer A, Green J, Pollard J Jr., Tugendreich S, Causal analysis approaches in Ingenuity Pathway Analysis, Bioinformatics 30 (2014) 523–530. 10.1093/bioinformatics/btt703. [PubMed: 24336805]

[23]. Tsvetkov L, Stern DF, Phosphorylation of Plk1 at S137 and T210 is inhibited in response to DNA damage, Cell Cycle 4 (2005) 166–171. 10.4161/cc.4.1.1348. [PubMed: 15611664]

[24]. Pal-Ghosh R, Xue D, Warburton R, Hill N, Polgar P, Wilson JL, CDC2 Is an Important Driver of Vascular Smooth Muscle Cell Proliferation via FOXM1 and PLK1 in Pulmonary Arterial Hypertension, Int J Mol Sci 22 (2021). 10.3390/ijms22136943.

[25]. Wang L, Guo Q, Fisher LA, Liu D, Peng A, Regulation of polo-like kinase 1 by DNA damage and PP2A/B55α, Cell Cycle 14 (2015) 157–166. 10.4161/15384101.2014.986392. [PubMed: 25483054]

[26]. Wakida T, Ikura M, Kuriya K, Ito S, Shiroiwa Y, Habu T, Kawamoto T, Okumura K, Ikura T, Furuya K, The CDK-PLK1 axis targets the DNA damage checkpoint sensor protein RAD9 to promote cell proliferation and tolerance to genotoxic stress, Elife 6 (2017) e29953. 10.7554/eLife.29953. [PubMed: 29254517]

[27]. van Vugt MATM, Gardino AK, Linding R, Ostheimer GJ, Reinhardt HC, Ong S-E, Tan CS, Miao H, Keezer SM, Li J, Pawson T, Lewis TA, Carr SA, Smerdon SJ, Brummelkamp TR, Yaffe MB, A mitotic phosphorylation feedback network connects Cdk1, Plk1, 53BP1, and Chk2 to inactivate the G(2)/M DNA damage checkpoint, PLoS Biol 8 (2010) e1000287–e1000287. 10.1371/journal.pbio.1000287. [PubMed: 20126263]

[28]. Montaudon E, Nikitorowicz-Buniak J, Sourd L, Morisset L, El Botty R, Huguet L, Dahmani A, Painsec P, Nemati F, Vacher S, Chemlali W, Masliah-Planchon J, Château-Joubert S, Rega C, Leal MF, Simigdala N, Pancholi S, Ribas R, Nicolas A, Meseure D, Vincent-Salomon A, Reyes C, Rapinat A, Gentien D, Larcher T, Bohec M, Baulande S, Bernard V, Decaudin D, Coussy F, Le Romancer M, Dutertre G, Tariq Z, Cottu P, Driouch K, Bièche I, Martin LA, Marangoni E, PLK1 inhibition exhibits strong anti-tumoral activity in CCND1-driven breast cancer metastases with acquired palbociclib resistance, Nat Commun 11 (2020) 4053. 10.1038/s41467-020-17697-1. [PubMed: 32792481]

[29]. Jia Z, Nie Y, Yue F, Kong Y, Gu L, Gavin TP, Liu X, Kuang S, A requirement of Polo-like kinase 1 in murine embryonic myogenesis and adult muscle regeneration, Elife 8 (2019). 10.7554/eLife.47097.

[30]. Coxon CH, Bicknell KA, Moseley FL, Brooks G, Over expression of Plk1 does not induce cell division in rat cardiac myocytes in vitro, PLoS One 4 (2009) e6752. 10.1371/journal.pone.0006752. [PubMed: 19707596]

[31]. Lindqvist A, Rodríguez-Bravo V, Medema RH, The decision to enter mitosis: feedback and redundancy in the mitotic entry network, J Cell Biol 185 (2009) 193–202. 10.1083/jcb.200812045. [PubMed: 19364923]

[32]. Bryce Y, Bourguillon R, Vazquez JC, Ziv E, Kim D, Santos Martin E, Prevalence, Outcome, and Management of Risk Factors in Patients With Breast Cancer With Peripheral Arterial Disease: A Tertiary Cancer Center's Experience, Clin Breast Cancer (2020). 10.1016/j.clbc.2020.12.010.

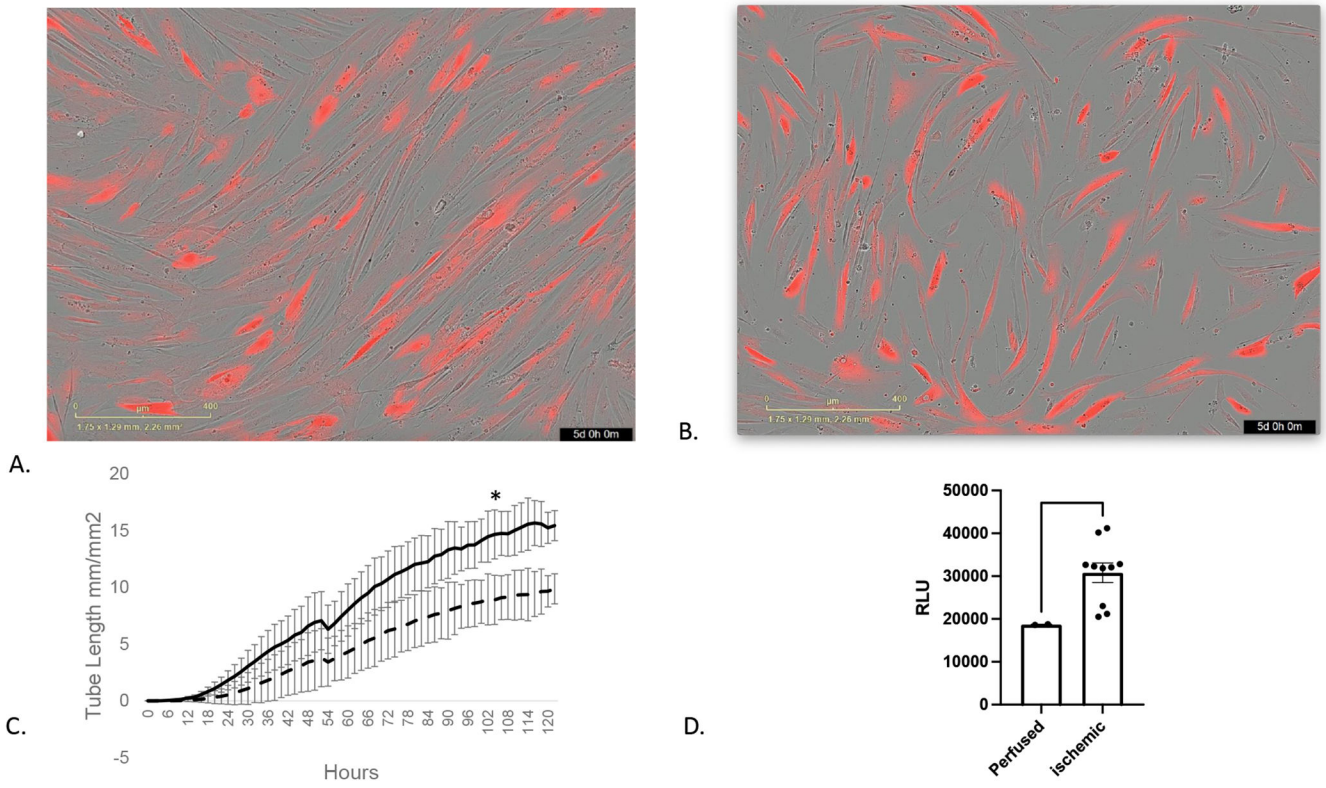

Figure 1 –. Myoblasts in PAD form comparatively short myotubes when induced to undergo fusion despite higher proliferation.

Incucyte® live cell imaging was used to automatically calculate the overall length of myocyte networks as a measure of myoblast fusion over five days. Myoblasts harvested from proximal and distal segments of muscle affected by PAD (N=4) were compared to those from healthy controls obtained from a commercial source (N= 2) A. Final images of cells incubated with cytoplasmic specific detection reagent that had been visualized every two hours over five days to assess myocyte length in multiple areas as a measure of fusion. B. Tube length graphed over time for perfused (control) and ischemic (PAD) cells. Error bars represent standard error of the mean (SEM); *p<0.03 (t-test) after 104 hours. C. Luminescence was used to evaluate proliferation of myoblasts from perfused and ischemic muscle segments. Despite shorter myotube lengths, proliferation was higher in ischemic cells (*p<0.05).

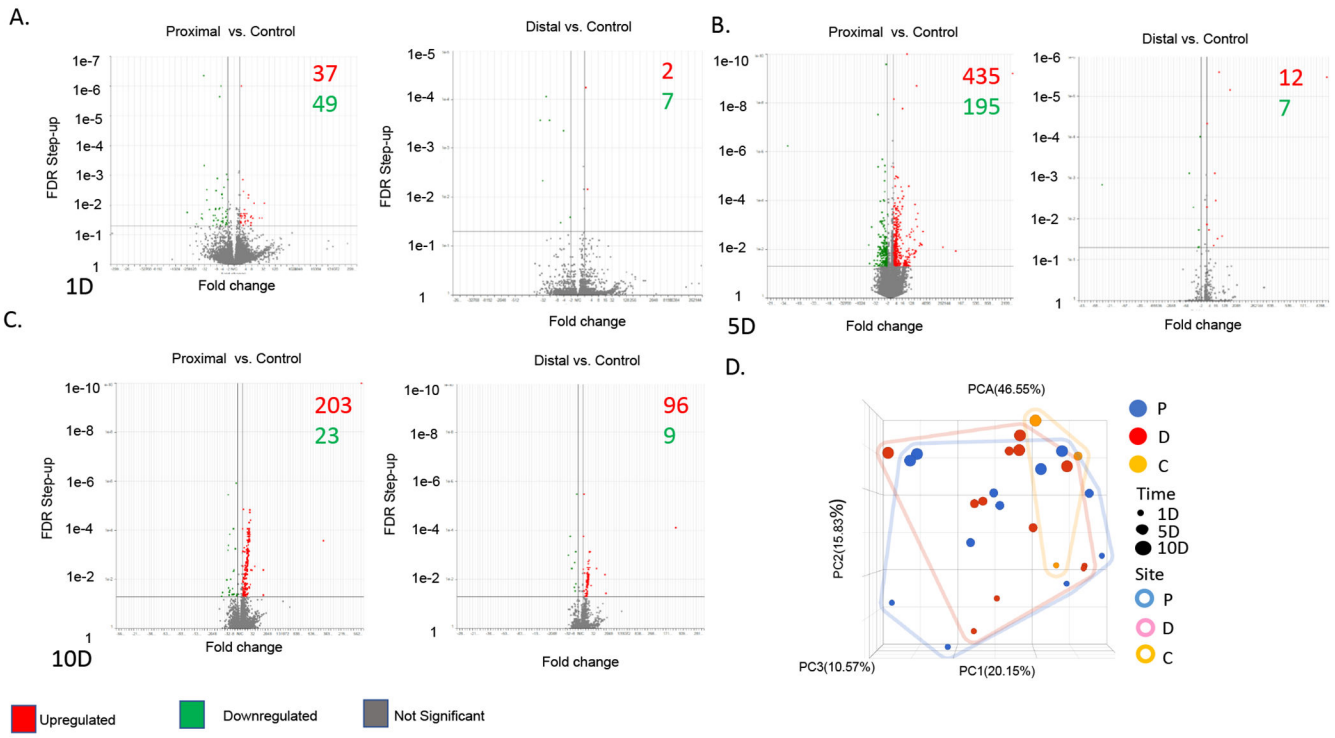

Figure 2 –. Myoblasts in PAD differ significantly in gene expression associated with cell cycle regulation.

Bulk RNA sequencing from proximal and distal segments of PAD muscle (N=4) and healthy controls (N= 2) was performed. Volcano plots demonstrate differential gene expression between control, proximal and distal myoblasts after 1 day of proliferation (A), 5 days of differentiation (B) and 10 days of differentiation (C). The number of differentially expressed genes are shown in each plot. D. PCA demonstrates significant differences among each sample at each time point.

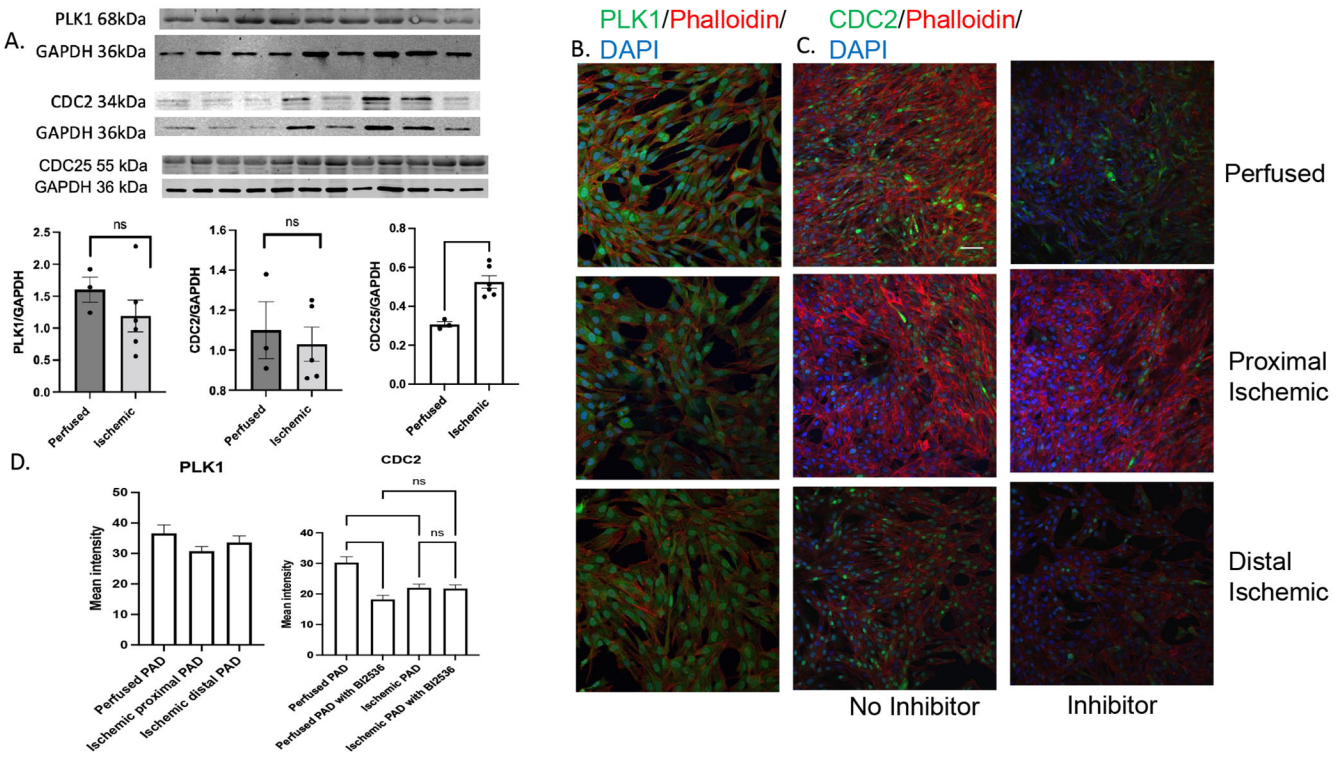

Figure 3 –. CDC2 expression is attenuated in PAD.

A. Immunoblotting for PLK1, CDC2 and CDC25 were performed on myoblasts lysates from both perfused (N=3) and ischemic (N=4-5) samples. Semi-quantitative measurements of expression was performed using Image J, normalizing to the housekeeping protein GAPDH (**p<0.006). Additionally, immunofluorescence was used to detect PLK1 (B) and CDC2 +/− BI2536 (C) expression in perfused(quadriceps) and ischemic (proximal and distal TA) myoblasts (N= 5 images/sample, N=3/samples each). D. Mean fluorescence intensity per unit area demonstrated for PLK1 and CDC2 ** p<0.006, two-way ANOVA with post-hoc t-test.

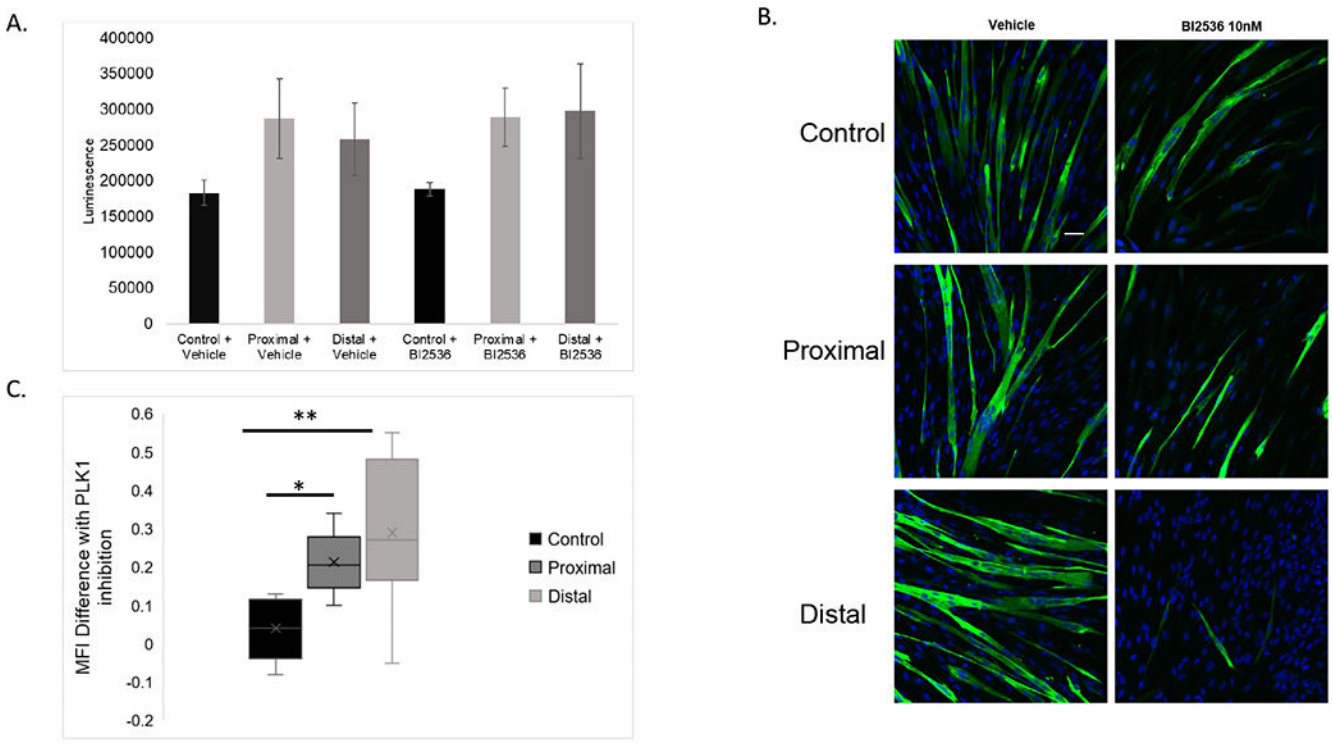

Figure 4 –. PLK1 plays a more significant role in myocyte differentiation in PAD compared to control myoblasts.

Myoblasts were incubated with either BI2536 (10nM) or DMSO vehicle and allowed to differentiate over 5 days. A. MF20 (green) and DAPI (blue) detected myosin heavy chain positivity and nuclear location, respectively, for control and PAD cells. B. Following calculation of MFI for each group with and without B12536, the absolute difference in MFI for inhibitor and vehicle treated cells was determined and compared using ANOVA with Holms-Sidak post hoc analysis, *p<0.03, **p<0.001. C. Cell viability over 24 hours of incubation with BI2536 was assessed using luminescence.